Transport and Communications Science Journal, Vol. 74, Issue 4 (05/2023), 530-543

Transport and Communications Science Journal

INFLUENCES OF INJECTOR GEOMETRY PARAMETERS ON FUEL INJECTION CHARACTERISTICS AND PARAMETERS OF A DIESEL ENGINE

Thin Quynh Nguyen[1,*], Duc Le Hoai[1], Dunin A.Y[2]

[1]Faculty of Mechanical Engineering, University of Transport and Communications, No 3 Cau Giay Street, Hanoi, Vietnam

[2]Faculty of Heat Engineering and Automotive Engines, Moscow Automobile and Road Construction State Technical University (MADI), 64, Leningradsky Prosp., Moscow, 125319, Russia

ARTICLE INFO

TYPE: Research Article
Received: 31/01/2023
Revised: 10/04/2023
Accepted: 12/04/2023
Published online: 15/05/2023
https://doi.org/10.47869/tcsj.74.4.12

[*] *Corresponding author*
Email: thinquynh@utc.edu.vn; Tel: +848 6661 9228

Abstract. Internal combustion engines (ICEs), especially diesel engines, continue to play a huge role in the development of the global economy. The research trends to improve combustion is still the main research direction in recent years with the help of 3D simulation tools. In this study, a 3D-model of a four-stroke, single-cylinder diesel engine was built using AVL Fire software to evaluate the influence of injector geometry parameters on engine characteristics. The results have shown that, with the injection pressure reaching 3000 (bar), and the turbocharger pressure maintained at 0.15 (MPa), the engine achieves the maximum power and the minimum brake fuel consumption when the angle between the axis of the nozzle hole and the axis of the fuel injection nozzle is 150 degrees. However, at this angle value, the soot emission value is the lowest but the nitrogen oxides (NO_x) value is close to reaching the maximum. Hydrocarbon (HC) and carbon monoxide (CO) emissions are the lowest value at 155 degrees of the angle between the axis of the spray hole and the axis of the fuel injection nozzle. Besides, the study also evaluated the engine's parameters when changing the injector hole diameter. With an injection hole diameter of 0.24 (mm), the maximum engine power increased by 5.3%, and the brake-specific fuel consumption decreased by 7.2% compared to other values of injection hole diameter. However, the engine emissions are not the best values in this case.

Keywords: 3000 bar, common rail, the geometry of fuel injection, diesel engine, AVL fire.

1. INTRODUCTION

The internal combustion engine still plays a crucial role in the world economy. Besides the main advantages such as maintenance, repair, economy, size, etc., the ICE still has a huge problem which is emissions to the environment. In addition, there is the problem of depletion of fossil fuel resources. Over the years, the research of ICEs has followed the trends to improve the working process of the engine including the main directions: redesign the engine, improve the working performance of systems and structures which optimizes their structure and working process; research new fire models with more advanced features fire models such as Homogeneous Charge Compression Ignition (HCCI), Reactivity Controlled Compression Ignition (RCCI), Premixed Charge Compression Ignition (PCCI), etc.; find biofuels and lubricating materials; find solutions to treat engine exhaust gases, example Exhaust Gas Recirculation (EGR), Selective Catalytic Reduction (SCR), Diesel Particulate Filter (DPF), etc. Finally, the control technique to optimize the working process and engine operation is studied and widely applied [1, 2].

The common rail system improves fuel injection and combustion in internal combustion engines. Since its appearance, the Common Rail (CR) system has also continuously developed and improved. The new research for CR systems has increased the injection pressure [3–6], and the number of injections in a cycle and followed the desired shape. In addition, fuel distribution in the combustion chamber can be applied [7, 8].

The different fuel injection rules are determined by the electromagnetic control pulse installed and were suitable for each operating mode of the engine. With various pressures, the working conditions as well as the parameters of the injection process are also adjusted accordingly [9]. In improving research on the CR system, especially multiple injections, the wave hammer problem in the high-pressure line of the fuel pipeline also needs to be noted. This pressure wave phenomenon will directly affect the quality of the fuel injection and the engine operation [10].

Studies have shown that the geometrical parameters of the spray are directly related to the fuel injection pressure as well as the shape of the combustion chamber. Besides, the geometrical parameters of the nozzle are also directly affected by the geometric parameters of the injectors such as the diameter of the injector hole, the cone angle of the injector hole, etc. Therefore, it is necessary to have studies on the development of the spray when changing the geometrical parameters of the injectors under high-pressure conditions for design and manufacture [11–15].

In this study, the influence of nozzle geometry parameters (including nozzle hole diameter and the angle between the axis of the nozzle hole and the axis of the injection nozzle) on the characteristics of the spray as well as the engine parameters of a diesel four-stroke, single cylinder is presented. The study is carried out through the use of a 3D simulation model on AVL Fire software. The fuel injection pressure was used in the model at 3000 bar, and the turbocharger pressures are maintained at 1.5 bar.

2. 3D MODEL IN AVL FIRE

2.1. Combustion model

The Extended Coherent Flame Model-3Z (ECFM - 3Z) combustion model was developed by Groupement Scientifique Moteurs (GSM) specifically for combustion calculation in diesel engines. This is a combustion model based on a flame surface density transport equation and a

mixing model that can describe the formation of inhomogeneous turbulent premixed and diffusion combustion. The model is based on the ECFM combustion model, described and implemented below in FIRE and described over 3 mixing zones. Furthermore, it is combined with an improved burnt gas chemistry description compared to ECFM. Zones in the ECFM-3Z model are shown in Fig. 1 [16].

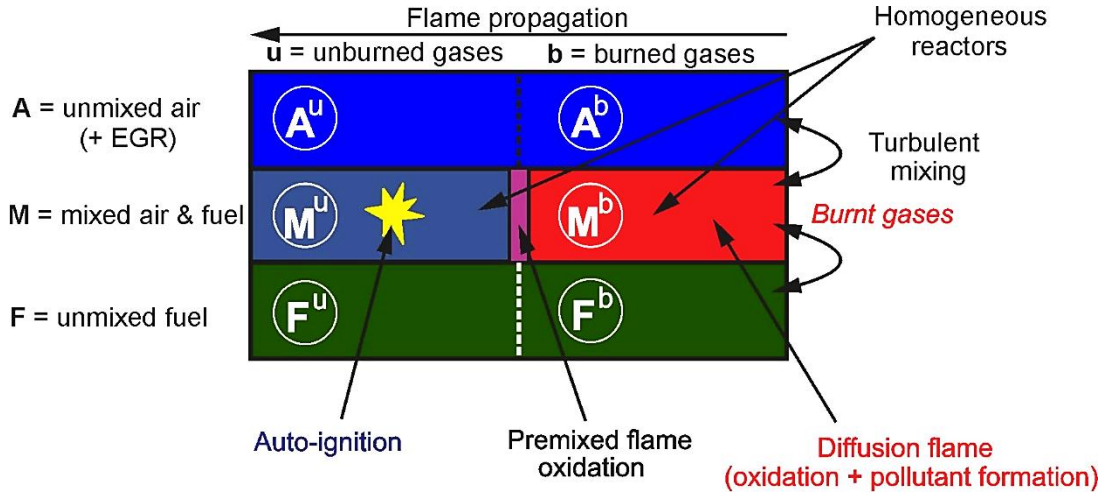

Figure 1. Zones in ECFM-3Z Model [16]

In the ECFM-3Z model, the transport equations are solved for the averaged quantities of chemical species O_2, N_2, CO_2, CO, H_2, H_2O, O, H, N, OH and NO. Here, averaged means these quantities are the global quantities for the three mixing zones (that is in the whole cell).

Therefore, the term "burnt gases" includes the real burnt gases in the mixed zone (zone M^b in Fig. 1) plus a part of the unmixed fuel (zone F^b in Fig. 1) and air (zone A^b in Fig. 1). This equation is classically modeled as:

$$\frac{\partial \bar{\rho}\tilde{y}_x}{\partial t} + \frac{\partial \bar{\rho}\tilde{u}_i\tilde{y}_x}{\partial x_i} - \frac{\partial}{\partial x_i}\left(\left(\frac{\mu}{Sc} + \frac{\mu_t}{Sc_t}\right)\frac{\partial \tilde{y}_x}{\partial x_i}\right) = \bar{\dot{\omega}}_x \quad (1)$$

where: $\bar{\dot{\omega}}_x$ is the combustion source term

$\widetilde{y_x}$ is the averaged mass fraction of species α

Sc_t - Turbulent Schmidt Number

$$Sc_t = \frac{\vartheta_t}{K}$$

ϑ_t is the eddy viscosity in units of (m^2/s)

K is the eddy diffusivity (m^2/s).

The fuel is divided in two parts: $\tilde{y}_{Fu}^u$ – the fuel present in the fresh gases, and $\tilde{y}_{Fu}^b$ – the fuel present in the burnt gases

$$\tilde{y}_{Fu} = \tilde{y}_{Fu}^u + \tilde{y}_{Fu}^b \quad (2)$$

$\bar{\rho}$ is mean density

Sc Schmidt number. It is defined as:

$$Sc = \frac{\vartheta}{D} = \frac{\mu}{\rho D} \quad (3)$$

where:

ϑ is the kinematic viscosity or (μ/ρ) in units of (m^2/s)

D is the mass diffusivity (m^2/s)

μ is the dynamic viscosity of the fluid (Pa·s or N·s/m^2 or kg/m·s)

μ_t is turbulent viscosities

ρ is the density of the fluid (kg/m^3).

2.2. Principles of NO Formation

In engines, the cylinder pressure rises during the combustion process, so earlier burnt gases are compressed to a higher temperature level as they are immediately after their combustion. Hence, the thermal NO formation in the burnt gases always dominates in comparison to the NO formed in the flame front and represents the main source of the nitric oxide in engines whose reaction paths are effective at high temperatures (> 1800 [K]). The reaction mechanism can be expressed in terms of the so-called extended Zeldovich mechanism:

$$N_2 + O \underset{k_{1b}}{\overset{k_{1f}}{\leftrightarrow}} NO + N \quad (4)$$

$$N + O_2 \underset{k_{2b}}{\overset{k_{2f}}{\leftrightarrow}} NO + O \quad (5)$$

$$N + OH \underset{k_{3b}}{\overset{k_{3f}}{\leftrightarrow}} NO + H \quad (6)$$

The first reaction represents the rate-limiting step in comparison to the other reactions. A very high activation energy (or temperature) is necessary to decompose the stable triple bond of the molecular air-nitrogen. Accordingly, this reaction is significantly fast at high temperatures (hence thermal). In principle, it can be seen that the thermal nitric oxide formation is mainly determined by only six chemical species (O, H, OH, N, N_2, and O_2) but not by the fuel being used. In order to obtain the required concentrations of the radicals, a complex reaction mechanism must be used in order to determine NO concentration. In the literature, different possibilities are suggested to represent the rate law for NO.

The first two reactions (Eq. 4- Eq. 5) were originally proposed by Zeldovich and extended later by including the third reaction (Eq. 6). It was observed later that the nitrogen atoms released at the reaction (Eq. 5) are oxidized to nitric oxide mainly by hydrogen radicals at near-stoichiometric conditions and in fuel-rich mixtures. The third reaction (Eq. 6) is usually negligible except in fuel-rich flames.

The reaction mechanism (Eq. 4-Eq. 6) is known as the extended Zeldovich mechanism that considers the effect of oxygen, nitrogen, and hydrogen radicals on NO formation. It is very important to point out that all three chemical reactions that represent the Zeldovich mechanism show strong temperature dependency [17].

2.3. Soot Formation

Under high temperatures and fuel-rich conditions, as typically found in diesel combustion, hydrocarbon fuels exhibit a strong tendency to form carbonaceous particles - soot. Usually, under engine running conditions, most of the soot formed in the early stages of the combustion process is depleted due to oxidation. This takes place in oxygen-rich areas of the combustion chamber later in the engine cycle. In diesel engines, it is the amount and completeness of the soot oxidation process that actually determines the engine particle emission characteristics.

The formation of particulates involves a large number of different chemical and physical processes, like the formation and growth of large aromatic hydrocarbons, their subsequent conversion to particles, the coagulation of primary particles, and the growth of solid soot particles due to the accumulation of gaseous components.

The soot particle formation process is characterized by a gaseous-solid conversion, whereby the solid phase does not exhibit a uniform chemical and physical topology.

The basis of this model is a detailed chemical reaction scheme for the calculation of soot formation and oxidation. It combines the mechanisms of formation of polyaromatic hydrocarbons, and polyynes, two mechanisms of soot precursor formation due to condensation of polyaromatic and polyyne molecules, soot particle growth by the reactions of HACA mechanism and polyyne molecule addition, the mechanism of acetylene pyrolysis and pure carbon cluster formation, as well as the reactions of hydrocarbon (n-heptane) oxidation.

The complete detailed kinetic scheme of the soot formation process incorporates 1850 gas-phase reactions, 186 species, and 100 heterogeneous reactions with the participation of four ensembles of micro-heterogeneous particles of different types.

The current model contains a reduced number of species and reactions and has been developed in order to provide a computationally efficient kinetic overall soot model. The model can describe the behavior of soot formation and oxidation for different fuel classes. Exact reaction constants have been implemented for methane, propane, ethanol, n-heptane, and tetradecane. If the fuel which you have specified does not exactly match one of these species, FIRE™ decides automatically the best parameter set to be used.

The reaction mechanism which is applied in the soot formation model is below:

$$C_nH_m + \frac{n}{2}O_2 = nCO + \frac{m}{2}H_2 \quad (7)$$

$$H_2 + H_2 + O_2 = H_2O + H_2O \quad (8)$$

$$CO + CO + O_2 = CO_2 + CO_2 \quad (9)$$

$$CO + H_2O = CO_2 + H_2 \quad (10)$$

$$C_nH_m + C_nH_m = 2nC + mH_2 \quad (11)$$

$$C + C + O_2 = CO + CO \quad (12)$$

$$C + H_2O = CO + H_2 \quad (13)$$

The reaction parameters for the main soot formation reaction are changing due to the local equivalence ratio. The soot is oxidized due to the presence of oxygen and also due to water [17].

2.4. The k-zeta-f Model

This model was developed by Hanjalic, Popovac and Hadziabdic (2004). The authors propose a version of eddy-viscosity model based on Durbin's elliptic relaxation concept (1991). The aim is to improve the numerical stability of the original $\overline{v^2} - f$ model by solving a transport equation for the velocity scale ratio $\zeta = \overline{v^2}/k$ instead of velocity scale $\overline{v^2}$. The full model is given below:

The eddy-viscosity is obtained from

$$v_t = C_\mu \zeta \frac{k^2}{\varepsilon} \tag{14}$$

and the rest of variables from the following set of model equation, thus

$$\rho \frac{Dk}{Dt} = \rho(P_k - \varepsilon) + \frac{\partial}{\partial \mathrm{x}_j}\left[\left(\mu + \frac{\mu_t}{\sigma_k}\right)\frac{\partial \mathrm{k}}{\partial \mathrm{x}_j}\right] \tag{15}$$

$$\rho \frac{D\varepsilon}{Dt} = \rho \frac{(C_{\varepsilon 1}^* P_k - C_{\varepsilon 2}\varepsilon)}{T} + \frac{\partial}{\partial \mathrm{x}_j}\left[\left(\mu + \frac{\mu_t}{\sigma_k}\right)\frac{\partial \varepsilon}{\partial \mathrm{x}_j}\right] \tag{16}$$

$$\rho \frac{D\zeta}{Dt} = \rho f - \rho \frac{\zeta}{k} P_k + \frac{\partial}{\partial \mathrm{x}_j}\left[\left(\mu + \frac{\mu_t}{\sigma_\zeta}\right)\frac{\partial \zeta}{\partial \mathrm{x}_j}\right] \tag{17}$$

where:

ε: turbulent diffusion,

k: turbulent kinetic energy

τ: turbulent time scale,

P_k turbulent kinetic energy

S: Modulus of the mean rate-of-strain

where the following form of the *f* equations as adopted

$$f - L^2 \frac{\partial^2 f}{\partial \mathrm{x}_j \partial \mathrm{x}_j} = \left(C_1 + C_2 \frac{P_k}{\zeta}\right)\frac{\frac{2}{3} - \zeta}{T} \tag{18}$$

and the turbulent time scale T and length scale L are given by

$$T = max\left(min\left(\frac{k}{\varepsilon}, \frac{a}{\sqrt{6C_\mu |S|\zeta}}\right), C_T\left(\frac{\upsilon}{\varepsilon}\right)^{1/2}\right) \tag{19}$$

$$L = C_L max\left(min\left(\frac{k^{3/2}}{\varepsilon}, \frac{k^{1/2}}{\sqrt{6C_\mu |S|\zeta}}\right), C_\eta \frac{\upsilon^{3/4}}{\varepsilon^{1/4}}\right) \tag{20}$$

The following values for the coefficients used in the equations are taken. C_μ = 0.22, σ_ζ = 1.2, σ_k = 1, c_1 = 1.4, C_2 = 0.65, $C_{\varepsilon 1}$ = 1.4(1+0.012/ ζ, $C_{\varepsilon 2}$ = 1.9, C_T = 6, C_L = 0.36 and C_η = 85.

Additional modifications to the ε equation that the constant $C_{\varepsilon 1}$ is dampened close to the wall thus

$$C_{\varepsilon 1}^* = C_{\varepsilon 1}\left(1 + 0.045\sqrt{1/\zeta}\right) \tag{21}$$

This is computationally more robust than the original model $\overline{v^2} - f$

In addition, sub-models employed are shown in Tab. 1 [16].

Table 1. AVL-FIRE Sub-Models [1, 18, 19]

Spray model	Wave
Spray wall interaction model	Walljet1
Droplet Evaporation model	Dukowicz
Turbulence model	k-zeta-f
Ignition model	Auto - ignition
NO formation	Extended Zeldovich
Soot formation	Kinetic

2.5. Simulation object and initial conditions

The engine used in the simulation is a single-cylinder engine, with a displacement of approximately 1.47 (l) and a compression ratio of 15.4: 1. The engine is located at the Engine Laboratory at Moscow Automobile and Road Construction State Technical University (MADI). Other specifications of the engine, input conditions, and boundary conditions of the simulation model are shown in Tables 2 and 3.

Table 2. Engine Specifications [1, 18, 19]

Parameter	Value
Bore, (mm)	120
Stroke, (mm)	130
Connecting rod length, (mm)	224
Number of cylinders (-)	1
Displacement, (l)	1.47
Compression ratio (-)	15.4
Number of valves (-)	4
Number of nozzle holes (-)	8
Nozzle hole diameter, (mm)	0.1

Table 3. Initial and boundary conditions [1, 18, 19]

Parameter	Value
Engine speed, (rpm)	1400
Intake air temperature, (K)	307
Cylinder head temperature, (K)	550.15
Piston top temperature, (K)	575.15
Fuel injection temperature, (K)	330.15
Cylinder wall temperature, (K)	475.15

The geometry of the combustion chamber is shown in Figure 2.

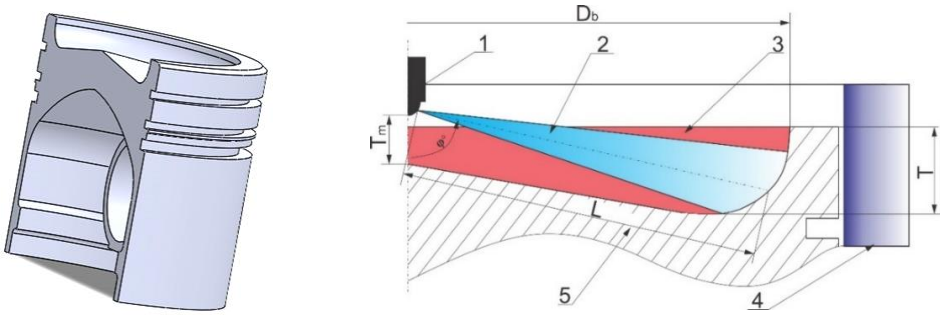

(**a**) (**b**)

Figure 2. Geometry of piston bowl shape: (a) 3D piston; (b) Basic parameters of the piston. 1—Nozzle; 2—Spray; 3—Combustion chamber; 4—Cylinder; 5—Piston.

Figure 3 illustrates the fuel injection rate used in the formula dq/dt = f(t). The fuel injection rate was determined experimentally with the fuel injection pressure of 3000 bar and the fuel injection value of 60 mg.

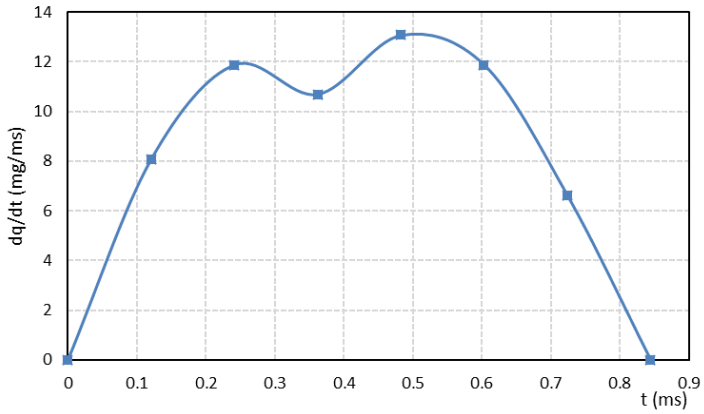

Figure 3. The fuel injection rate used in the model (p_{ij} = 3000 bar, Q_c = 60 mg).

2.6. Simulation methods and conditions

The engine model runs at 1400 rpm, and the turbocharger pressure is maintained at 0.15 MPa. Nozzle diameter was investigated at five values in Table 5. The angle between the axis of the spray hole and the axis of the fuel injection nozzle is investigated at five values in Table 4. During the simulation study, the engine model used has a constant compression ratio (ε = 15.4), and the shape of the combustion chamber is as shown in Figure 2. In addition, the fuel injection angle is also kept at a constant value of 5 degrees before Top Dead Center (TDC).

3. THE RESEARCH RESULTS AND DISCUSSION

3.1. Validation of a 3D combustion model in AVL Fire

To validate the combustion model (Tables 2 and 3) in the AVL Fire, the values of the in-cylinder pressure and Rate of Heat Release (RoHR) were compared to those in an experiment. According to the results received in Automobile and Road State Technical University (MADI), with a mean effective pressure at 9 bar, engine speed at 1400 rpm, and a fuel injection angle at 23° crank angle (CA) before TDC, the maximum combustion pressure in the combustion cylinder is 84 (bar), and the maximum value of the RoHR is 48 (J/deg.CA) with 1500 (bar) of injection pressure. The results are shown in Figure 4. The experimental RoHR is determined through Lab-view software (single zone + heat transfer).

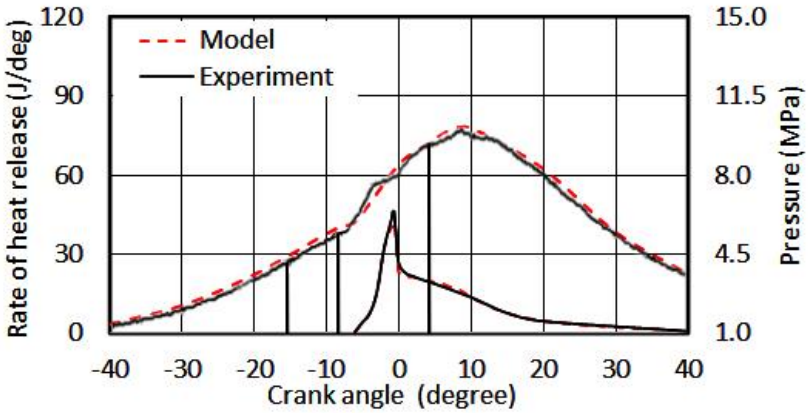

Figure 4. Validation of the AVL Fire model with the experimental results

The results show that the average error between the modeling and the experimental results are less than 5%; therefore, this model can be used in studying the impact of different parameters on the diesel engine combustion process.

3.2. Effect of the angle between the axis of the spray hole and the axis of the fuel injection nozzle on engine parameters

The γ angle is the angle between the axis of the nozzle hole and the axis of the injector as shown in Figure 5.

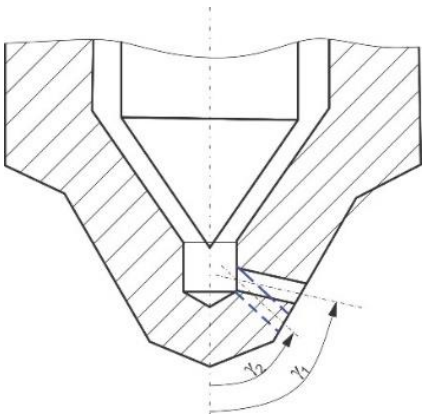

Figure 5. Determine the gamma (γ) angle

The smaller the γ angle is, the longer the nozzle hole increases, and the more the injection fuel sprays into the piston head. In contrast, fuel was injected into the clearance area between the piston and the cylinder head. Therefore, the γ angle affects the fuel distribution area in the combustion chamber. In this study, five angle values are considered which show in Table 4.

Table 4. Cases of the γ angle

Case	γ
1	140
2	145
3	150
4	155
5	160

The indicated power, indicated specific fuel consumption as well as emissions of the engine are shown in Figures 6, 7.

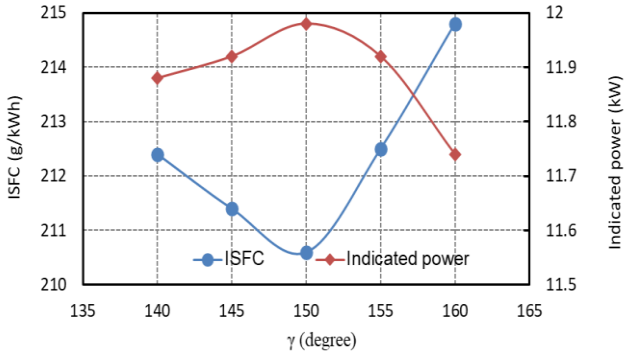

Figure 6. Dependence of indicated power and indicated specific fuel consumption (ISFC) on the gamma angles

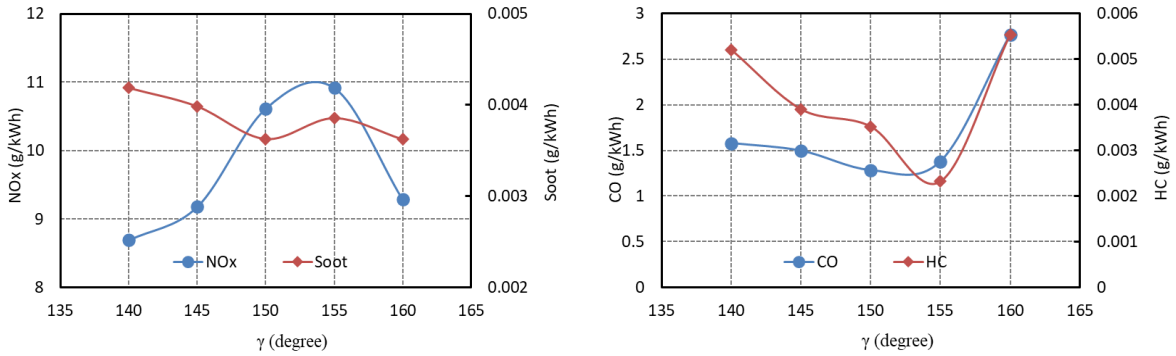

Figure 7. Dependence of exhaust emissions on the gamma angles

From the results obtained as shown in Figures 6 and 7, it can be seen that the engine has the maximum power and the lowest fuel consumption when the γ angle is at 150°. Indicated power value increases by 2%, the ISFC decreases by 2% compared to the case of the γ angle at 160°. However, at this value of the γ angle, the engine emissions are not the best. The soot value is the minimum but the NOx value is close to the maximum value. In addition, the HC emission is the minimum, the CO value is close to the minimum when the γ angle is at 155°. Therefore, if the choice of engine power is the main factor, the γ angle should be chosen at 150° for the case study.

It is also important that due to the nozzle hole diameter being 0.1 mm, the Start of Injection (SOI) also is adjusted to close to the TDC. Through optimizing the SOI, which also is chosen at TDC. With this injection angle, the engine power is the highest and the fuel consumption is the lowest.

The change in emission values and the ISFC is the result of the amount of fuel dropping on the cylinder wall and the piston bowl when the gamma angle is changed. With large or small gamma angles (cases 1, 2, and 5), the amount of fuel that will inject into the cylinder wall increases. These fuels will need time and heat to evaporate during the first stage of combustion and finally, the combustion time of the first stage increases. With the injection angle unchanged in the model, the combustion process is pushed back to the BDC, so the engine powers are low, and the ISFC is high. In addition, the amount of HC, CO, and PM increases.

3.3. Effect of nozzle hole diameter on engine parameters

Based on the selection of the optimal γ angle, the influence of the nozzle hole diameter on the

engine parameters was also studied. Five values of the nozzle hole diameters are studied (Table 5).

Table 5. Value of the nozzle hole diameter

Case	d
1	0.10
2	0.15
3	0.19
4	0.24
5	0.32

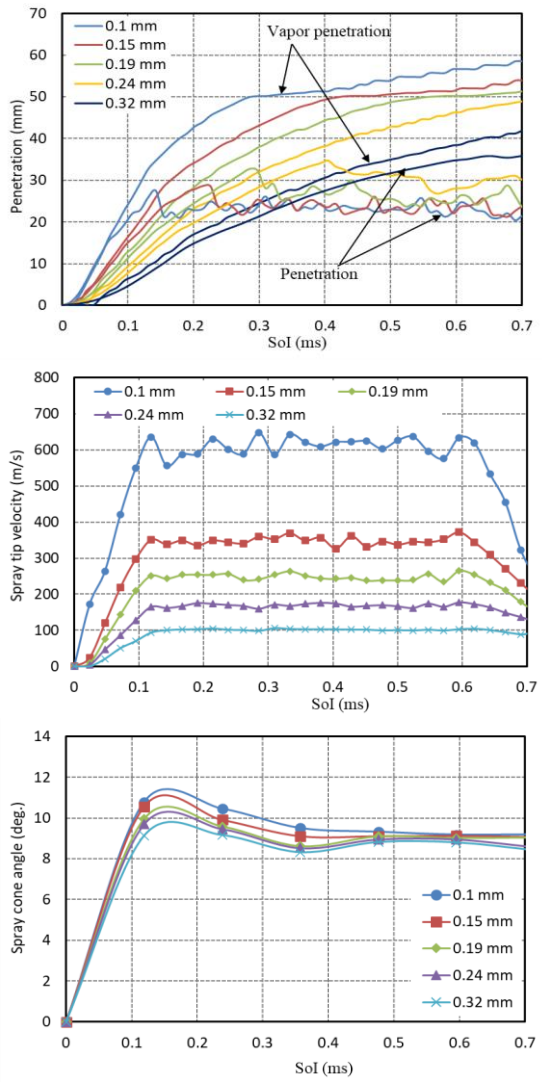

Figure 8. Characteristics of spray when changing the nozzle hole diameter

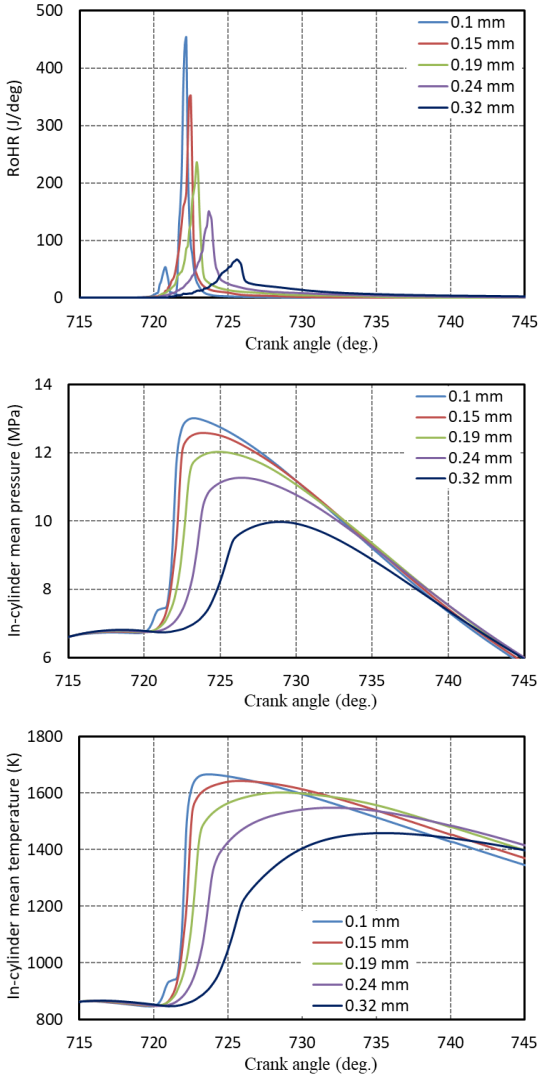

Figure 9. Rate of heat release (RoHR), pressure and temperature in cylinder when changing the nozzle hole diameter

The indicated power, ISFC, and exhaust emissions are shown in Figures 10 and 11. In principle, the SOI is adjusted when changing the nozzle hole diameter which ensures obtaining the maximum indicated power or the minimum exhaust emissions. This problem depends on each specific research. In this case, the SOI was set at 5 degrees before the TDC corresponding to the original engine when using an injection with a nozzle hole diameter of 0.24 mm and an

injection pressure of 300 MPa.

The results show that the indicated power and ISFC of the engine depend on the nozzle hole diameter. When changing the nozzle hole diameters, the maximum indicated power changes up to 5.3% and the ISFC up to 7.2% with 300 MPa of the injection pressure and 0.15 MPa of the turbocharger pressure. As the injector hole diameter decreases, the fuel particles are smaller than that in the condition of ultra-high injection pressure, and the fuel sprays are concentrated on the position of the injection hole. In addition, because the pressure of the turbocharger is also small (0.15 MPa), the fuel spray area is very large.

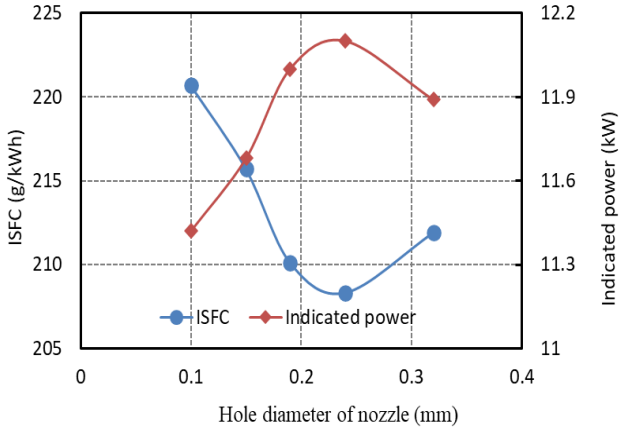

Figure 10. ISFC and indicated power of the engine when changing the nozzle hole diameter

As a result, the amount of air in the combustion chamber still exists in areas that are far from the nozzle and the combustion takes place mainly near the nozzle. In these cases, the injector hole value with a diameter of 0.24 mm gives the maximum indicated power, and the smallest ISFC, but has a relatively large NO_x emission (Figure 11).

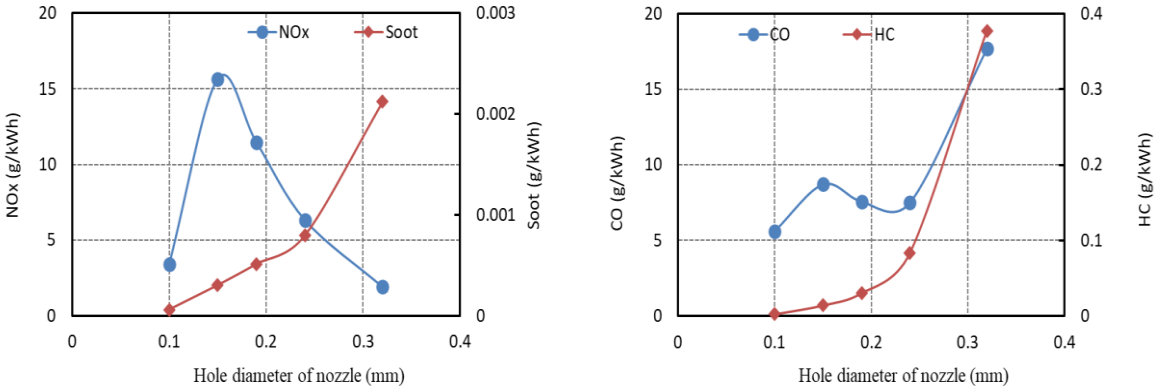

Figure 11. NO_x and CO of the engine when changing the nozzle hole diameter

It is well-known that the NO_x value depends on the amount of oxygen in the combustion chamber, the combustion temperature, and the possibility of contacting oxygen and nitrogen in the combustion chamber. In the study, the maximum amount of NO_x at the nozzle diameter is 0.19 mm. At this nozzle hole diameter, the burning area is the largest. Besides, the amount of oxygen in the combustion chamber is used more when compared to the nozzle with a diameter

of 0.1 mm.

As for HC and CO emissions, the higher the injection pressure is, the smaller the fuel particles with a small nozzle diameter. As a result, the HC and CO values in the exhaust gas are reduced. In contrast, the fuel particle size grows up when the nozzle hole diameter increases. In addition, the fuel spray length also increases, and the amount of fuel injected onto the wall of the combustion chamber increases. The sum of all these factors leads to high CO and HC emissions.

4. CONCLUSION

This study has created a simulation model of a diesel single-cylinder engine using AVL fire software. The model was evaluated for accuracy before assessing the influence of the nozzle hole diameter and the angle between the axis of the nozzle hole and the axis of the injector on engine characteristics. Qualitative and quantitative analysis of the research results suggests the following conclusions:

- The engine has the maximum power and the minimum fuel consumption when the γ angle is at 150^o. However, at this value of the γ angle, the soot value is the minimum but the NOx value is close to the highest value. In addition, the HC emission is the best, the CO value is close to the lowest when the γ angle is at 155^o. Therefore, if the choice of engine power is the main factor, the γ angle should be chosen at 150^o for the case study.

- When changing the nozzle hole diameters, the maximum indicated power changes up to 5.3% and the ISFC up to 7.2% with 300 MPa of the injection pressure and 0.15 MPa of the turbocharger pressure. The injector hole value with a diameter of 0.24 mm gives the best indicated power and the lowest ISFC. However, the emissions of NO_x, soot, HC, and CO are still relatively high values. It can be seen that the optimization problem between power, fuel consumption, and exhaust emissions is still a huge challenge.

ACKNOWLEDGMENT

This research is funded by University of Transport and Communications (UTC) under grant number T2023-CK-004TĐ

REFERENCES

[1]. N. T. Quynh, M. G. Shatrov, L. N. Golubkov, A. Y. Dunin, P. V. Dushkin, Influence of Injection Pressure and Pressure Oscillation and on the Rate of Fuel Outflow from the Sprayer of an Electrohydraulic Diesel Nozzle, in Wave Electronics and its Application in Information and Telecommunication Systems (WECONF), (2021). https://doi.org/10.1109/WECONF51603.2021.9470538

[2]. A. Y. Dunin, N. T. Quynh, L. N. Golubkov, Computational Study of the Effect of Increasing the Fuel Injection Pressure Up to 3000 Bar on the Performance of the Diesel Engine and its Gaseous Emissions, in 2020 International Conference on Engineering Management of Communication and Technology (EMCTECH), Oct. 2020, pp. 65–70, https://doi.org/10.1109/10.1109/EMCTECH49634.2020.9261516

[3]. M. Palanisamy, J. Lorch, R. J. Truemner, B. Baldwin, Combustion Characteristics of a 3000 Bar Diesel Fuel System on a Single Cylinder Research Engine, SAE Int. J. Commer. Veh., 8 (2015) 479–490. https://doi.org/10.4271/2015-01-2798

[4]. J. Johnson, J. Naber, S. Y. Lee, G. Hunter, R. Truemner, T. Harcombe, Correlations of non-vaporizing spray penetration for 3000 bar diesel spray injection, in SAE Technical Papers, 11(2013) 12.

https://doi.org/10.4271/2013-24-0033
[5]. G. Boccardo, F. Milloa, A. Pianoa, L. Arnoneb, S. Manellib, S. Faggc, P. Gattic, O. Erik Herrmannd, D. Queckd, J. Weber, Experimental investigation on a 3000 bar fuel injection system for a SCR-free non-road diesel engine, Fuel, 243 (2019) 342–351. https://doi.org/10.1016/j.fuel.2019.01.122
[6]. A. Vidal, P. Koukouvinis, M. Gavaises, Effect of Diesel Injection Pressures up to 450MPa on In-nozzle Flow Using Realistic Multicomponent Surrogates, 29th Conf. Liq. At. Spray Syst., 8534 (2019) 0–3.
[7]. A. Y. Dunin, M. G. Shatrov, L. N. Golubkov, A. L. Yakovenko, Providing Boot-Type Injection Rate Shape by Electric Impulse Control of the Common Rail Injector, Proc. High. Educ. Institutions. Machine Build., 1(2020) 32–42. https://doi.org/10.18698/0536-1044-2020-1-32-42.
[8]. M. G. Shatrov, V. I. Malchuk, A. Y. Dunin, I. G. Shishlov, V. V. Sinyavski, A control method of fuel distribution by combustion chamber zones and its dependence on injection conditions, Therm. Sci., 22 (2018) S1425–S1434.
[9]. A. E. Catania, A. Ferrari, M. Manno, E. Spessa, Experimental investigation of dynamics effects on multiple-injection common rail system performance, J. Eng. Gas Turbines Power, 130 (2008) 032806.
[10]. M. G. Shatrov, L. N. Golubkov, A. Y. Dunin, P. V. Dushkin, Pressure Oscillations as a Factor Affecting the Management of the Fuel Injection Process in the Combustion Chamber of a Diesel Engine, 2019 Syst. Signals Gener. Process. F. Board Commun. SOSG, (2019) 1–5. https://doi.org/10.1109/SOSG.2019.8706808
[11]. L. Postrioti, G. Buitoni, F. C. Pesce, C. Ciaravino, Zeuch method-based injection rate analysis of a common-rail system operated with advanced injection strategies, Fuel, 128 (2014) 188–198. https://doi.org/10.1016/j.fuel.2014.03.006
[12]. L. Xu, X. S. Bai, M. Jia, Y. Qian, X. Qiao, X. Lu, Experimental and modeling study of liquid fuel injection and combustion in diesel engines with a common rail injection system, Appl. Energy, 230 (2018) 287–304. https://doi.org/10.1016/j.apenergy.2018.08.104
[13]. R. Balz, G. Bernardasci, B. von Rotz, D. Sedarsky, Influence of nozzle geometry on spray and combustion characteristics related to large two-stroke engine fuel injection systems, Fuel, 294 (2021) 120455. https://doi.org/10.1016/j.fuel.2021.120455
[14]. M. A. Quazi, S. K. Singh, M. Jadhao, Effect of piston bowl shape, swirl ratio and spray angle on combustion and emission in off road diesel engine, SAE Tech. Pap., 2015 (2015) 15.
[15]. S. J. M. Algayyim, A. P. Wandel, T. Yusaf, The impact of injector hole diameter on spray behaviour for butanol-diesel blends, Energies, 11 (2018) 1298. https://doi.org/10.3390/en11051298
[16]. AVL, AVL Fire Combustion user manual version 2022 - Combustion Module, AVL List GmbH: Austria, 2022.
[17]. AVL, FIRE_Emission user manual version 2022 - Emission Module, AVL List GmbH: Austria, 2022.
[18]. T. Q. Nguyen, Control the Combustion of Fuel Sprays in Power Plants, in 2021 International Conference on Engineering Management of Communication and Technology (EMCTECH), 2021, https://doi.org/10.1109/emctech53459.2021.9618982
[19]. A. Y. Dunin, N. T. Quynh, M. G. Shatrov, L. N. Golubkov, Analysis of the nozzle hole diameter effect to common rail diesel engine characteristics using a calculated model of an internal combustion engine, Int. J. Emerg. Trends Eng. Res., 8 (2020) 2301–2308. https://doi.org/10.30534/ijeter/2020/17862020